JACS Au
AN OPEN ACCESS JOURNAL OF THE AMERICAN CHEMICAL SOCIETY

Editors' Choice
Open Access

pubs.acs.org/jacsau

Article

Overexpression of a Designed Mutant Oxyanion Binding Protein ModA/WtpA in *Acidithiobacillus ferrooxidans* for the Low pH Recovery of Molybdenum and Rhenium

Heejung Jung, Virginia Jiang, Zihang Su, Yuta Inaba, Farid F. Khoury, and Scott Banta*

Cite This: *JACS Au* 2024, 4, 2957−2965

Read Online

ACCESS | Metrics & More | Article Recommendations | Supporting Information

ABSTRACT: Molybdenum and rhenium are critically important metals for a number of emerging technologies. We identified and characterized a molybdenum/tungsten transport protein (ModA/WtpA) of *Acidithiobacillus ferrooxidans* and demonstrated the binding of tungstate, molybdate, and chromate. We used computational design to expand the binding capabilities of the protein to include perrhenate. A disulfide bond was engineered into the binding pocket of ModA/WtpA to introduce a more favorable geometric coordination and surface charge distribution for oxyanion binding. The mutant protein experimentally demonstrated a 2-fold higher binding affinity for molybdate and 6-fold higher affinity for perrhenate. The overexpression of the wild-type and mutant ModA/WtpA proteins in *A. ferrooxidans* cells enhanced the innate tungstate, molybdate, and chromate binding capacities of the cells to up to 2-fold higher. In addition, the engineered cells expressing the mutant protein exhibited enhanced perrhenate binding, showing 5-fold and 2-fold higher binding capacities compared to the wild-type and ModA/WtpA-overexpressing cells, respectively. Furthermore, the engineered cell lines enhanced biocorrosion of stainless steel as well as the recovered valuable metals from an acidic wastewater generated from molybdenite processing. The improved binding efficiency for the oxyanion metals, along with the high selectivity over nontargeted metals under mixed metal environments, highlights the potential value of the engineered strains for practical microbial metal reclamation under low pH conditions.

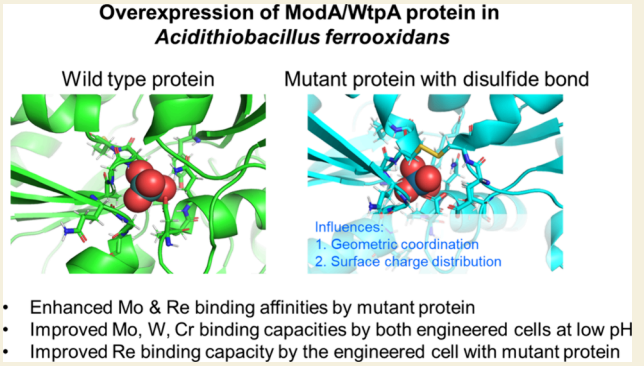

KEYWORDS: *Acidithiobacillus ferrooxidans, ModA, WtpA, Genetic engineering, Oxyanion metal binding, Molybdate, Tungstate, Perrhenate, Chromate*

INTRODUCTION

Trace elements can play important roles in cellular biochemistry;[1,2] however, they can also be potent inhibitors to cells at high concentrations. Many cells have adopted unique cellular transport systems, such as the adenosine triphosphate (ATP) binding cassette (ABC) transporter, to maintain the homeostasis of trace elements within the cells. Once transported through the cytoplasmic membrane, metals are used to synthesize cofactors, form metalloenzymes, and regulate metal-dependent transcription or translation and can be stored for future use.[3] Oxyanion metals, such as molybdate (MoO_4^{2-}) and tungstate (WO_4^{2-}), are essential micronutrients for most bacteria. These oxyanions can be transported intracellularly via tungsten and/or molybdenum transporter proteins (WtpABC, ModABC, or TupABC).

The flexibility of metal binding sites in proteins enables proteins to accommodate different metals having similar characteristics.[4] The metal-centered oxygens, molybdate and tungstate, have close structural and functional properties, including their ionic radii and free energy of solvation,[5] which allow them to be transported via the same molybdenum/tungsten transporters. Indeed, there is very little difference in the crystal structures of ModA and WtpA in coordination with molybdate or tungstate.[6] The molybdenum/tungsten transporters selectively bind with molybdate and tungstate over other tetrahedral oxyanions such as sulfate and phosphate,[5,7] while ModA and TupA can also bind chromate (CrO_4^{2-})[8,9] or perrhenate (ReO_4^-),[10] with lower affinities. Although no known biological function has been reported for rhenium, it is an exceptionally rare element on Earth[11] and has unique and valuable applications in various industries, enabling extraordi-

Received: April 2, 2024
Revised: May 2, 2024
Accepted: May 3, 2024
Published: July 13, 2024

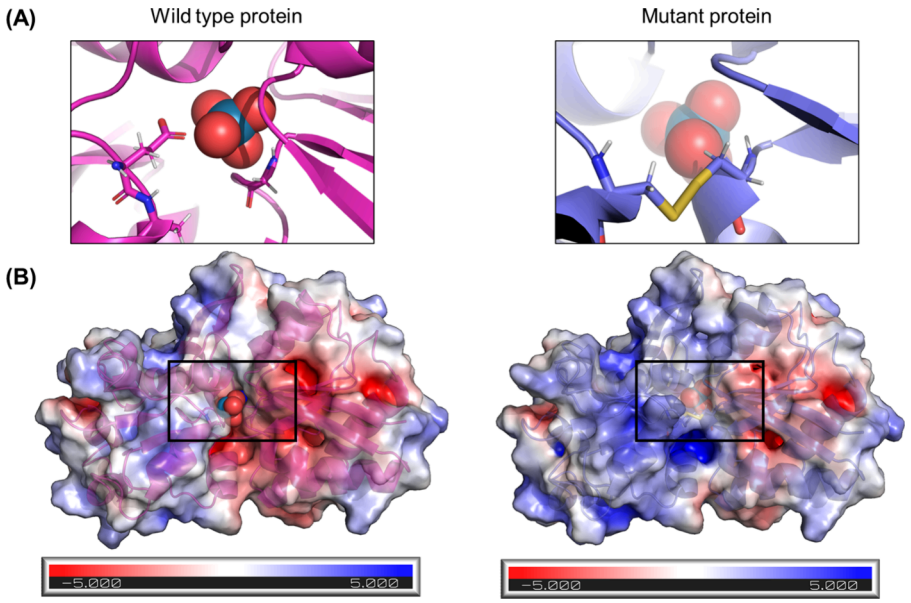

Figure 1. (A) Predicted three-dimensional structures of *A. ferrooxidans* wild-type and mutant proteins (AFE_1498) in coordination with tungstate and perrhenate, respectively. The new disulfide bond between G9C and A166C in the mutant protein is depicted in yellow. The designed disulfide is a +RH spiral with a dihedral angle of 91.5°. The structures were visualized using Pymol. (B) Predicted Poisson−Boltzmann electrostatic potentials for both proteins after oxyanion binding where the regions of positive (>+5 kT/e) and negative (<−5 kT/e) potentials are depicted by blue and red, respectively. Inset areas in panel A are shown by a black outline in panel B.

nary heat and acid resistance in alloys.[12] Therefore, there is growing interest in new routes for the recovery of this element.

A recent study reported the enhanced binding affinity of the *E. coli* ModA protein for perrhenate by introducing a new disulfide bond near the binding pocket.[4] Disulfide bonds, which are covalent linkages between two cysteine residues formed by oxidation of thiol groups, play an important role in maintaining the three-dimensional structure and stability of proteins. While disulfide bonds are known to contribute to the overall stability and folding of a protein,[13] they can also affect the local chemical environment, influencing the charge of the protein surface.[13−16] Although bacteria generally lack a mechanism for the formation of disulfide bonds in the cytoplasmic compartment, the expression of proteins with disulfide bonds in periplasmic space can occur due to a more oxidizing environment.[17,18] Previous studies have reported that the presence of a disulfide bond can increase ligand affinity by reducing conformational flexibility of the protein.[19,20] In accordance with this, the authors reported the enhanced perrhenate binding affinity of the mutant *E. coli* ModA occurred by preventing the rapid displacement of perrhenate by molybdate.[4]

The acidophilic extremophiles involved in industrial metal bioleaching thrive in harsh conditions including high concentrations of toxic metals.[21] *Acidithiobacillus ferrooxidans* is able to oxidize iron or sulfur and has been explored as a platform for biotechnology applications.[22] We have engineered these cells for critical metal reclamation applications by overexpressing recombinant proteins that enable divalent metal cation,[23] copper,[24] and rare earth element[25] recovery. A recent study described the purification of a periplasmic protein from *A. ferrooxidans* that exhibited specific tungstate binding under acidic conditions.[26] Given the low pH (2.5−3.0) in the periplasm of these cells, this protein holds promise for the recovery of oxyanion metals at low pH, providing an appealing route for the reclamation of valuable metals.[22]

Previous studies also reported the presence of multiple putative genes belonging to the ModA family in *A. ferrooxidans*.[27−29] However, the characterization of the oxyanion metal transporter proteins in *A. ferrooxidans* remains limited. We identified a gene sequence (AFE_1498) in *A. ferrooxidans* that shares approximately 30% identity with ModA/WtpA of *Pyrococcus horikoshii* (3CG3_A) and *P. furiosus* (3CG1_A), suggesting the potential involvement of this putative gene in metal-centered oxygen transfer. Understanding the molecular mechanisms underlying oxyanion metal transport in *A. ferrooxidans* is important, as we aim to explore adaptations and metal tolerance strategies that are used in extreme environments. Furthermore, characterization of a ModA/WtpA protein in *A. ferrooxidans* can provide insights into its potential for use in biotechnological applications, such as metal recovery and bioremediation.

Here, we characterized the oxyanion metal binding capability of the putative ModA/WtpA protein (AFE_1498) of *A. ferrooxidans* at low pH. This putative protein was found to bind molybdate, tungstate, and chromate, while an engineered *A. ferrooxidans* strain with overexpression of the protein improved the binding capacity for all tested oxyanions. Drawing inspiration from the previous mutations made in the *E. coli* ModA,[4] we further engineered this protein to expand its ability to bind perrhenate. The engineered cells with mutant protein demonstrated enhanced perrhenate binding, in addition to molybdate, tungstate, and chromate, at low pH. Finally, the engineered cells demonstrated enhanced metal recovery from industrial sources (stainless steel and a process concentrate), which showcases the applicability of the strains for practical metal reclamation.

RESULTS

Protein Characterizations

The three-dimensional structural models of the wild-type (AFE_1498) and the mutant proteins from *A. ferrooxidans*

https://doi.org/10.1021/jacsau.4c00296
JACS Au 2024, 4, 2957−2965

Table 1. Validation of Metal Binding Sites in Crystal Structures of the Wild-Type (AFE_1498) and Mutant (G9C/A166C) Protein for Molybdate (Mo), Tungstate (W), Chromate (Cr), and Perrhenate (Re), Analyzed by the CheckMyMetal (CMM) Server[a]

	wild-type protein				mutant protein			
	Mo	W	Cr	Re	Mo	W	Cr	Re
geometry	TB	OH	OH	TB	TB	OH	OH	TB
nVECSUM	0.01	0.3	0.34	0.1	0.06	0.18	0.22	0.06
pocket volume (Å^3)	148	148	184	148	95	107	105	97
Rosetta ddG	−5.5	−10	−5.5	−3.8	−8.1	−11	−5.4	−5.3

[a]Three-dimensional arrangements of ligands coordinated with metals are indicated as TB, trigonal bipyramidal; and OH, octahedral. nVECSUM shows the amplitude of the vector sum of bond valence vectors normalized by overall valence. Rosetta ddG was used as a protein−ligand interface score, which estimates of the binding energy of a complex.

were computed by RoseTTAFold, a three-track neural network that can rapidly predict the folded structures of proteins (Figure S1). The modeled wild-type protein consists of two similar domains (termed the N and C domains) connected by a flexible hinge loop, where the anion binding site is at the interface of the two domains. Similar to the experimentally solved ModA/WtpA structure from *A. fulgidus*, there is a beta hairpin loop between the two domains that is not present in the experimentally solved structures of the *E. coli* and *A. vinelandii* ModA/WtpA proteins. In the modeled *A. ferrooxidans* putative protein (AFE_1498), the oxyanion is coordinated by two key acidic residues in the binding site (D153 and E192), which confer distorted octahedral coordination of the tungstate and molybdate oxyanions. Both of these acidic residues are conserved in the *A. fulgidus* structures, but only one acidic residue is present in the binding pockets of the *E. coli* and *A. vinelandii* ModA/WtpA, which bind via tetrahedral coordination.

A disulfide design program in Rosetta (disulfidize)[30] was used to explore mutations of pairs of pocket residues to cysteines to identify the most energetically favorable disulfide bonds proximal to the oxyanion binding site in the wild-type protein model. The most favorable mutations were G9C and A166C (G26C and A193C, respectively, including signal peptides; Table S1), where G9C is in the N domain and A166C is in the C domain. Introducing this disulfide bond between the two lobes should stabilize the interface and reduce the flexibility of the hinge loop. Additionally, this disulfide bond would sterically shift one of the previously identified key acidic coordinating residues out of the anion binding pocket (E165; E192 when signal peptides are included), so that the mutant ModA/WtpA could bind an oxyanion with tetrahedral coordination. Perrhenate has been previously shown to bind with highest affinity to pockets with tetrahedral coordination.[4] In addition, the designed disulfide bond should cause a coil-to-helix transition in the metal binding site and connect the left and right lobes of the mutant protein (lobes B and A, respectively) to decrease the volume of the ion binding cavity[31] (Figure 1A). This structural shift should also decrease the solvent exposure of the ion in the binding pocket and create a tunnel of positive electrostatic potential that may help recruit the oxyanion to the protein (Figure 1B).

The metal binding residues found in the structures of the wild-type and mutant proteins were analyzed by CheckMyMetal server,[32] and evaluation parameters are presented in Table 1. The geometric arrangements of the proteins were predicted to improve for most of the tested metals when simulated with a mutant protein. The lower nVECSUM values predicted for the mutant protein suggests that the metal−ligand interactions would be closer to ideal geometries and symmetries.[32] In addition, the volume of the binding pocket of the mutant protein was predicted to decrease in comparison with the wild-type protein, for all tested metals. The metal−ligand interactions of both proteins were further evaluated by the standard Rosetta ddG score function in the server, which calculates the binding energy of protein−ligand complex.[33] The mutant protein with a designed disulfide bond improved the binding interface score for all tested metals while showing a comparable score for chromate, in comparison with the wild-type protein (Table 1).

Validation of Oxyanion Metal Binding by the Proteins

To validate the mutant protein design, the oxyanion metal binding abilities of the proteins were experimentally verified. The wild-type (AFE_1498) and mutant (G9C/A166C) proteins with C-terminal polyHis tags were expressed in *E. coli* and then purified using immobilized metal affinity chromatography followed by size exclusion chromatography (Figure 2A). The purified proteins were reacted with solutions containing molybdate, tungstate, chromate, or perrhenate at pH 1.8. Both the wild-type and mutant proteins bound nearly all of the molybdate, tungstate, and chromate in the solutions (Figure 2B). These results confirm that the putative protein (AFE_1498) is capable of binding oxyanion metals and will now be termed ModA/WtpA in *A. ferrooxidans*. The mutant protein also showed a high perrhenate binding efficiency (93% bound), whereas only a small fraction of the perrhenate (1.4%) was bound by the wild-type protein. These results confirm that the designed mutations in ModA/WtpA introduced a new perrhenate binding capability to the protein, without impacting the intrinsic binding affinities of the rest of the tested metals. Furthermore, both wild-type and mutant proteins showed insignificant binding with iron (1.7 ± 0.3% and 1.3 ± 0.5%, respectively; data not shown), showing the specificity of ModA/WtpA for the tested oxyanions.

We next explored the impact of the mutations on the thermal stability of the ModA/WtpA protein. The secondary structures were characterized by using circular dichroism (CD) spectroscopy. The mean residue ellipticity (MRE) at 208 and 222 nm was used to estimate the α-helical content in proteins, enabling the determination of the protein thermal stabilities as a function of temperature.[34] For the wild-type protein, the loss of α-helical content was observed starting at around 40−45 °C, whereas the mutant protein retained its stability at higher temperatures (>50 °C) (Figure 2C, Figure S2). The melting temperatures for both proteins were estimated as 45 ± 1 °C for the wild-type protein and 61 ± 1 °C (208 nm) and 70 ± 3 °C (222 nm) for the mutant protein, respectively (Figure S3).

https://doi.org/10.1021/jacsau.4c00296
JACS Au 2024, 4, 2957−2965

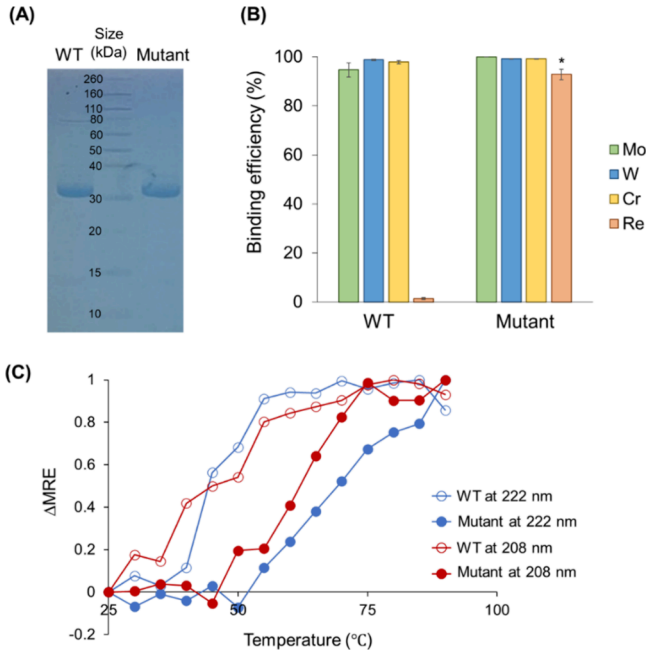

Figure 2. (A) SDS-PAGE image of wild-type (WT) and mutant (Mutant) proteins with polyHis tags, which were purified using Ni-NTA His-bind resin, followed by size exclusion chromatography. The protein sizes were estimated as 35 kDa for both proteins with polyHis tags. (B) Oxyanion binding efficiencies in solutions containing molybdate (Mo), tungstate (W), chromate (Cr), or perrhenate (Re) after 1 h binding experiment (pH 1.8) with the WT and Mutant proteins. The asterisk indicates statistical significance ($p < 0.05$) compared to the WT protein for the same type of metals. Error bars represent one standard deviation. (C) CD spectra of the purified proteins as a function of temperature. The changes of mean residue ellipticity (ΔMRE) of helix peaks at wavelengths of 208 and 222 nm are plotted as a function of temperature elevating from 25 to 90 °C.

The binding interactions of proteins and metals were further characterized by measuring the changes in the intrinsic fluorescence of tryptophan amino acids in the protein that occur upon binding of the oxyanions.[35] Reactions were performed with a fixed amount of purified proteins and different initial metal concentrations. Both wild-type and mutant ModA/WtpA proteins exhibited decreased fluorescence emission from the tryptophan residues upon binding of the metals. The final fraction of fluorescence quenching at varying metal concentrations was fitted with the Langmuir isotherm equation (Figure S4), which is a suitable model to interpret the interactions of oxyanions and the ModA/WtpA with a single metal binding site,[36] and dissociation constants were estimated (Table 2). The wild-type protein was estimated to have a K_d of 320 nM for molybdate, 490 nM for tungstate, and 500 nM for chromate, respectively. The mutations in the protein enhanced the binding affinity for molybdate, showing a 2-fold lower K_d value (150 nM), whereas the mutant protein maintained similar affinities for tungstate and chromate as compared to the wild-type ModA/WtpA. Furthermore, the mutant protein yielded a 6-fold lower K_d for perrhenate (160 nM) than the wild-type protein, which confirmed the mutation significantly enhanced the affinity for perrhenate, as was predicted by the modeling results (Table 2 and Figure S4).

Table 2. Estimated Dissociation Constants of Molybdate (Mo), Tungstate (W), Chromate (Cr), and Perrhenate (Re) As Measured Using Quenching of Intrinsic Tryptophan Fluorescence during Binding with the Purified Wild-Type and Mutant ModA/WtpA Proteins at pH 1.8

	dissociation constant (nM)	
metal	wild-type protein	mutant protein
Mo	320 ± 30	150 ± 10[a]
W	490 ± 110	360 ± 60
Cr	500 ± 110	480 ± 70
Re	1000 ± 100	160 ± 30[a]

[a]Statistical significance ($p < 0.05$) compared to the wild-type protein for the same type of metals.

Metal Binding Capability of the Engineered Strains with Synthetic Metal Solutions

After the binding affinities for molybdate, tungstate, chromate, and/or perrhenate were confirmed *in vitro* using the purified proteins, plasmids encoding the wild-type and mutant ModA/WtpA proteins were transformed into *A. ferrooxidans* cells (Table S2). The engineered strains exhibited higher transcriptional expression of the AFE_1498 gene, showing 4.4 × 10^9 copies/g cDNA and 4.1 × 10^9 copies/g cDNA by the recombinant (over)expression of wild-type and mutant proteins, respectively, compared to the wild-type cell (3.5 × 10^8 copies/g cDNA) (data not shown). Once the expression of the transgenes was verified, the oxyanion metal binding capabilities of engineered *A. ferrooxidans* strains were evaluated. The engineered strains with (over)expression of wild-type and mutant ModA/WtpA were referred to as AF_{WP} and AF_{MP}, respectively. The (over)expression of these proteins did not impact the core metabolism of *A. ferrooxidans*, including iron oxidation (Figure S5).

Pure Metal Solutions. Metal binding capabilities of the wild-type and engineered strains with molybdate, tungstate, chromate, and perrhenate were initially tested using pure metal solutions (pH 1.8) with 1 mM concentration, considering the tolerance of *A. ferrooxidans* for the tested oxyanions.[37−39] All of the strains were found to bind molybdate, tungstate, and chromate, which is unsurprising given that the ModA/WtpA protein is endogenously expressed in *A. ferrooxidans* (Figure 3). Both of the engineered cell lines further enhanced the binding capacities of the cells for all tested oxyanion metals, and the enhanced binding capacity for molybdate, tungstate, and chromate was comparable between the two engineered cells. Compared to the wild-type cells, both engineered strains showed 1.4-fold higher binding capacity for molybdate (18 fg/cell for both AF_{WP} and AF_{MP}), 2-fold higher capacity for tungstate (0.23 fg/cell for AF_{WP} and 0.24 fg/cells for AF_{MP}), and 1.3-fold higher capacity for chromate (0.6 fg/cell for both AF_{WP} and AF_{MP}). On the other hand, AF_{MP} cells had a higher perrhenate binding capacity of 1.3 fg/cell, which were 5- and 2-fold higher than the wild-type and AF_{WP} cells, respectively. Consistent with the *in vitro* results, both engineered cells enhanced the molybdate, tungstate, and chromate binding of the native cells, while the cells with the mutant protein exhibited a unique enhanced binding affinity for perrhenate. Meanwhile, the tested strains did not show significant binding capacity to other oxyanion metals, including phosphate and arsenite (Figure S6).

Mixed Metal Solutions. Reactions with mixed metal solutions containing the four oxyanion metals and iron were

https://doi.org/10.1021/jacsau.4c00296
JACS Au 2024, 4, 2957−2965

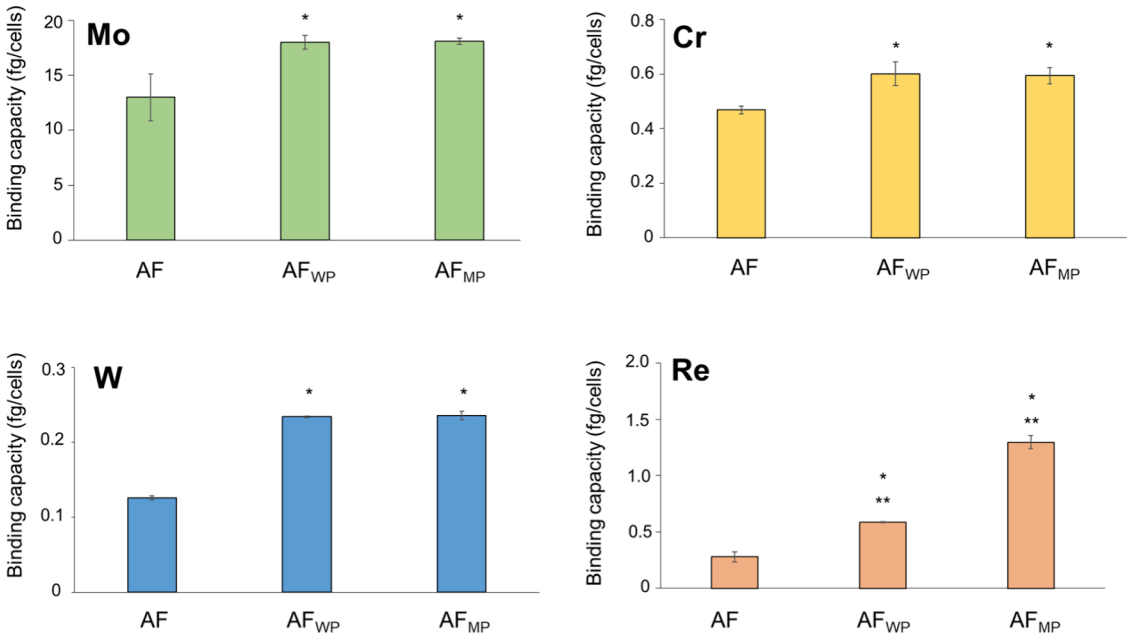

Figure 3. Metal binding capacities for molybdate (Mo), tungstate (W), chromate (Cr), and perrhenate (Re) of the wild-type (AF) and engineered *A. ferrooxidans* with (over)expression of the wild-type (AF$_{WP}$) and mutant (AF$_{MP}$) ModA/WtpA proteins. Reactions were made with 1 mM pure metal solutions at pH 1.8. Error bars represent the standard deviation. The asterisks indicate statistical significance ($p < 0.05$) compared to the wild type (AF, *) and between the engineered strains (AF$_{WP}$ and AF$_{MP,}$ **).

performed, and the binding capacities were all decreased in the wild-type and engineered cells compared to the pure metal solution (Figure 4). The comparable binding capacity for iron

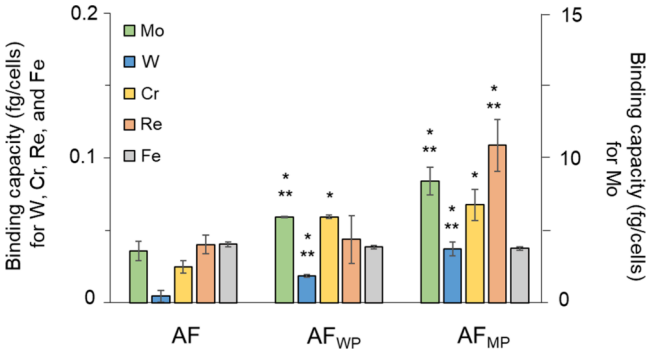

Figure 4. Metal binding capacities for molybdate (Mo), tungstate (W), chromate (Cr), perrhenate (Re), and iron (Fe) of the wild-type (AF) and engineered *A. ferrooxidans* with (over)expression of the wild-type (AF$_{WP}$) and mutant (AF$_{MP}$) ModA/WtpA proteins. Reactions were performed with 1 mM of a mixed metal solution containing molybdate, tungstate, perrhenate, and iron, at pH 1.8. Error bars represent standard deviation. The asterisks indicate statistical significance ($p < 0.05$) compared to the wild-type (AF, *) and between the engineered strains (AF$_{WP}$ and AF$_{MP,}$ **).

among the strains (0.04 fg/cell) indicates nonspecific binding for iron. While all strains exhibited the greatest uptake of molybdate, both engineered strains showed higher binding capacities for molybdate (5.9 fg/cell for AF$_{WP}$ and 8.4 fg/cell for AF$_{MP}$), tungstate (0.02 fg/cell for AF$_{WP}$ and 0.04 fg/cell for AF$_{MP}$), and chromate (0.06 fg/cell for AF$_{WP}$ and 0.07 fg/cell for AF$_{MP}$), in comparison with wild-type AF (3.6 fg/cell for molybdate, 0.05 fg/cell for tungstate, and 0.03 fg/cell for chromate). For perrhenate, the AF$_{MP}$ cells resulted in 2.7-fold higher binding capacity than the wild-type AF and AF$_{WP}$ cells. Overall, these results demonstrate that the overexpression of ModA/WtpA protein in *A. ferrooxidans* effectively increased the molybdate, tungstate, and chromate binding capability from both pure and mixed metal solutions and that engineering the cells with the mutant protein further enabled perrhenate binding.

Engineered Cells for Valuable Metal Reclamation

Molybdenum and Rhenium Recovery from Process Concentrate. While industrial sources containing rhenium are rare, the acidic wastewater generated from the washing and extraction steps of porphyry molybdenite processing contains molybdenum and rhenium as major components (see Materials and Methods section). To evaluate the potential value of the new strains for recovery of valuable metals from waste materials, the engineered cells were reacted with diluted process concentrates (pH 1.6), and the metal recovery efficiency was compared with the wild-type AF cells. In accordance with the binding results using synthetic metal solutions, both engineered cells showed improved recovery efficiency of molybdenum or rhenium from the solution. Compared to the wild-type AF cells, AF$_{WP}$ and AF$_{MP}$ cells recovered 2-fold more molybdenum, while the AF$_{MP}$ also recovered 3-fold more rhenium than the wild-type and AF$_{WP}$ cells (Table 3). The higher intracellular content of molybdenum and/or rhenium in the AF$_{WP}$ and AF$_{MP}$ cells supported the enhanced binding of these metals by the engineered strains (Figure S7). Meanwhile, both AF and AF$_{MP}$ cells showed nonspecific binding with selenium and arsenic, which were present in the process concentrate, during the reactions (data not shown).

Biocorrosion and Metal Reclamation

Stainless steels are generally resistant to acid corrosion, and we have recently developed methods and culture conditions for enhancing the biocorrosion of stainless steels by *A. ferrooxidans*.[40,41] The introduction of pyrite and sulfur and

https://doi.org/10.1021/jacsau.4c00296
JACS Au 2024, 4, 2957−2965

Table 3. Efficiency of Molybdenum and Rhenium Recovery from Diluted Acidic Wastewater Generated from Porphyrin Molybdenite Processing (pH 1.6) after a Binding Experiment Using the Wild-Type (AF) and Engineered *A. ferrooxidans* with (Over)expression of the Wild-Type (AF_{WP}) and Mutant (AF_{MP}) ModA/WtpA Proteins[a]

	AF	AF_{WP}	AF_{MP}
molybdenum	6.0 ± 0.1%	12 ± 1%*	12 ± 1%*
rhenium	1.7 ± 0.1%	1.9 ± 0.2%*,**	5.7 ± 0.1%*,**

[a]The asterisks indicate statistical significance ($p < 0.05$) compared to the wild type (AF, *) and between the engineered strains (AF_{WP} and AF_{MP}, **).

overexpression of the *rus* gene were used to enhance the corrosion of SS316, which is a high-grade chromium−nickel stainless steel containing molybdenum (Table S3). We have previously found SS316 to be resistant to acid corrosion under abiotic conditions (data not shown). Since SS316 contains chromium and molybdenum, we hypothesized that the engineered strains expressing ModA/WtpA may also enhance corrosion and could serve a dual role for the reclamation of these valuable metals included in the steel alloys. To explore this, the biocorrosion of SS316 coupons was performed with the new engineered cells, in the absence of pyrite. After 6 days of biocorrosion, the wild-type and engineered cells induced corrosion of the SS316 coupons. Both engineered cell lines enabled enhanced corrosion, and they induced more substantial passivation layers (sulfur content of 5%, 17%, and 24% for AF, AF_{WP}, and AF_{MP}, respectively; data not shown) and pits on the surface (Figure S8A and B). This is in contrast with the wild-type AF cells, where the surfaces of coupons were relatively intact,[42] and less surface passivation was observed (Figure S8B). These observations were consistent with the mass decreases of the coupons by the different cells, which achieved 1.9%, 4.8%, and 9.4% by AF, AF_{WP}, and AF_{MP}, respectively (Figure 5A). In addition to enhancing the corrosion rates, the cells absorbed the metals solubilized from the coupons during the corrosion. The concentrations of molybdenum and chromium in the leaching solutions were significantly lower in the experiments with both engineered cells (<0.3 mg/L for Mo and ca. 0.1 mg/L for Cr) as compared to the wild-type cells (4 mg/L for Mo and 0.5 mg/L for Cr) (Figure 5B). The higher molybdenum and chromium binding by the engineered cells matched the higher concentrations of these metals associated with the cells as determined by SEM-EDS (Figure S8C). These results demonstrate that both engineered cells can accelerate corrosion of stainless steel while simultaneously binding and sequestering the leached molybdenum and chromium.

DISCUSSION

The presence of metal-centered oxygens in molecular structures enables the metals to exhibit various oxidation and coordination numbers, which confers high electrostatic and redox activities.[43−45] These distinctive characteristics of these oxyanion metals endow them versatility and value, which explains their increasing use in a wide range of material, biochemical, energy, and environmental applications. Here, an uncharacterized protein (AFE_1498) in *A. ferrooxidans* was recombinantly expressed and purified for the first time, and the oxyanion metal binding of the protein was characterized. This new ModA/WtpA protein may be homologous to the protein

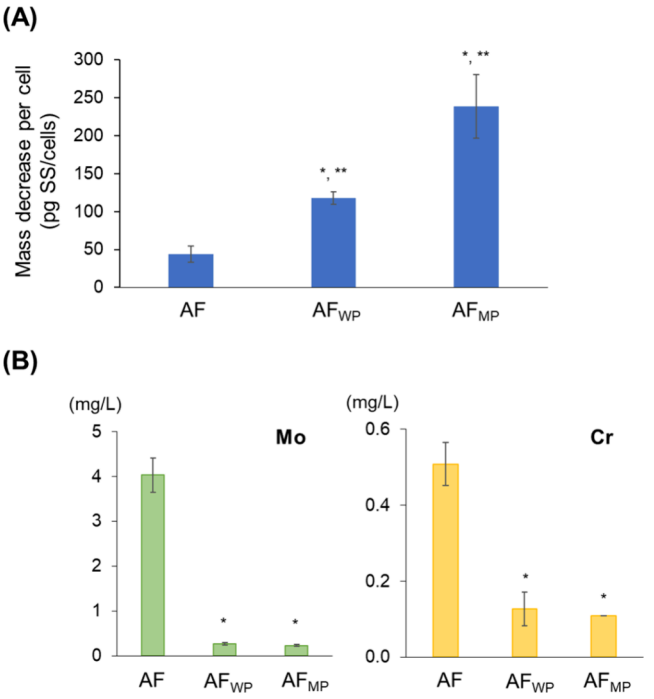

Figure 5. (A) Mass decreases in SS316 coupons normalized by cells and (B) the concentrations of molybdenum and chromium remaining in the solutions after biocorrosion. The biocorrosion was performed with the wild-type (AF) and engineered *A. ferrooxidans* with (over)expression of ModA/WtpA (AF_{WP}) and mutant ModA/WtpA (AF_{MP}) for 6 days. Error bars represent standard deviations. The asterisks indicate statistical significance ($p < 0.05$) compared to the wild type (AF, *) and between the engineered strains (AF_{WP} and AF_{MP}, **).

that has previously been reported to enable tungstate binding in a different *A. ferrooxidans* strain.[26]

A disulfide bond was previously introduced into the *E. coli* ModA protein,[4] and we hypothesized a similar approach could be taken with the new *A. ferrooxidans* ModA/WtpA protein. Computational modeling was consistent with experimental results, where we observed more favorable binding with the disulfide bond-containing mutant protein in coordination with the tested oxyanion metals (molybdate, tungstate, chromate, and perrhenate), in terms of the geometric arrangement and surface charge distribution of the metal−protein complexes (Table 1 and Figure 1). The volume of the binding pocket in the mutant protein was predicted to be reduced (Table 1), which is closer to the minimum van der Waals radius for binding oxyanions.[46] The binding scores of the mutant ModA/WtpA protein were estimated to significantly increase when binding to perrhenate. This prediction was confirmed when a high degree of perrhenate binding (94%) was experimentally observed by the purified mutant protein, while both purified proteins showed over 95% binding efficiency for the rest of the metals (Figure 2B). The protein simulation results suggested that the cysteine mutations and subsequent disulfide bond would affect the structural characteristics of the protein (Figures 1B and 2C). The results of the CD analyses agree with this prediction, as the disulfide bond likely restricted flexibility in the pocket volume of the mutant protein, increasing its thermal stability. Finally, the variations in the geometric arrangements caused by the disulfide bond likely influence the orientation of the charged residues around the

https://doi.org/10.1021/jacsau.4c00296
JACS Au 2024, 4, 2957−2965

binding pocket of the mutant protein, creating favorable local environments for electrostatic interactions with oxyanion metal ions.[15,16]

It is noteworthy that the mutant protein could bind to all of the tested oxyanions, which have different protonation states in mixed metal solutions. At pH 1.8, the majority of molybdate, tungstate, and chromate are likely protonated (pK_a, 3.8 for molybdate; 6.7 for tungstate; and 6.5 for chromate),[4,47] whereas perrhenate (pK_a, −1.25)[47] is likely in deprotonated form. This suggests that the protonation state was not a major determinant for oxyanion metal binding in mutant ModA/WtpA, but more likely determined by the local environment around the binding pocket induced by conformational change, as discussed above. This is supported by a previous study which observed that *Azotobacter vinelandii* ModA discriminates molybdate over sulfate by modulating the pocket size, rather than charge of metals.[46] The authors also proposed that the ligands in the protein can arrange local dipoles to make up for the uncompensated charges on bound metals, suggesting that the binding of metals with different charges is not unreasonable.

Disulfide bonds are rare in bacteria due to the reducing environment of the cytosol. It is significant to note that the improved oxyanion binding and additional perrhenate binding were observed in the engineered cells with the mutant protein, AF_{MP} (Figure 3). As ModA/WtpA protein is expressed in periplasm, an oxidizing compartment, the cysteines in the mutant protein should be able to form a disulfide linkage.

The engineered cells show potential for practical applications for metal reclamation from industrial sources. The two engineered cells recovered targeted metals (molybdenum, chromium, and/or rhenium) over nontargeted metals either from the porphyry molybdenite processing concentrates or stainless steel (SS) coupons. The binding selectivity of each cell was determined by using the elemental ratio from the SEM-EDS results. Compared to the wild-type AF cells, the AF_{WP} and AF_{MP} cells showed higher target-to-nontarget ratio in the reactions of process concentrates (target metals = Mo and Re; 0.008 for AF and 0.014 for AF_{WP} and AF_{MP}) and SS coupons (target metals = Mo and Cr; 0.023 for AF, 0.15 for AF_{WP}, and 0.34 for AF_{MP}) (Figures S7 and S8). This indicates the high selectivity of the engineered cells for the tested oxyanion metals against nontargeted metals in the industrial wastes. Interestingly, both engineered cells caused more corrosion on the SS316 coupons than the wild-type cells (Figures 5A and S8). We previously enhanced biocorrosion of the same SS316 coupons with the wild-type *A. ferrooxidans* cells by adding pyrite and/or sulfur.[40,41] If we assume a constant rate of corrosion to compare experiments, the newly engineered cells in this work (especially AF_{MP}) not only outperformed the biocorrosion we previously reported but also did so in the absence of pyrite and/or sulfur and also effectively sequestered the solubilized metals from the coupons. The increased surface pitting and the formation of sulfur passivation layers[48] (Figure S8B) by the engineered cells may be linked to their enhanced binding for molybdate and chromate, which will be further investigated. In addition to the enhanced metal recovery at low pH, the simultaneous leaching and recovery of metals from solid wastes by the engineered cells could be advantageous for the practical use of these cells.

These results highlight the potential value of engineered microbial systems to address pressing environmental concerns such as the depletion of critical metals and the accumulation of industrial wastes. The enhanced binding and selectivity for oxyanions hold promise for industries reliant on efficient metal reclamation processes, where the extraction of specific metals from complex waste streams is paramount. Our findings offer a sustainable approach to industrial metal reclamation, contributing to the development of environmentally friendly technologies for metal recovery and recycling.

CONCLUSION

The low pH binding of oxyanion metals by the putative ModA/WtpA protein of *A. ferrooxidans* (AFE_1498) was demonstrated for the first time. The wild-type protein bound molybdate, tungstate, and chromate, while the mutant protein increased perrhenate binding affinity via the introduction of a disulfide bond in the binding pocket. The enhanced binding capacities of the oxyanions were also observed by the engineered *A. ferrooxidans* with (over)expression of the wild-type and mutant proteins in synthetic metal solutions. Both engineered cells showed higher selectivities for the tested oxyanions over nontarget metals, under the mixed metal environment including industrial wastes. These observations demonstrate how protein design can be used to create novel binding interactions that can be leveraged for applications such as the recovery of valuable oxyanion metals in genetically engineered extremophiles.

ASSOCIATED CONTENT

Supporting Information

The Supporting Information is available free of charge at https://pubs.acs.org/doi/10.1021/jacsau.4c00296.

Materials and methods, protein primary sequences, bacterial strains and plasmids used, composition of the SS316 stainless steel coupons, 3-D protein structure models, circular dichroism (CD) spectra and CD spectra as a function of temperature, tryptophan fluorescence data for determining dissociation constants, *A. ferrooxidans* growth curves, *A. ferrooxidans* binding of phosphate and arsenite, elemental compositions of *A. ferrooxidans* cells by SEM-EDS, and images and elemental compositions of the stainless steel coupons (PDF)

AUTHOR INFORMATION

Corresponding Author

Scott Banta − *Department of Chemical Engineering, Columbia University, New York, New York 10027, United States;* orcid.org/0000-0001-7885-0150; Phone: +1 212 854 7531; Email: sbanta@columbia.edu; Fax: +1 212 854 3054

Authors

Heejung Jung − *Department of Chemical Engineering, Columbia University, New York, New York 10027, United States*

Virginia Jiang − *Department of Chemical Engineering, Columbia University, New York, New York 10027, United States*

Zihang Su − *Department of Chemical Engineering, Columbia University, New York, New York 10027, United States;* orcid.org/0000-0001-6216-6880

https://doi.org/10.1021/jacsau.4c00296
JACS Au 2024, 4, 2957−2965

Yuta Inaba − *Department of Chemical Engineering, Columbia University, New York, New York 10027, United States*
Farid F. Khoury − *Department of Chemical Engineering, Columbia University, New York, New York 10027, United States;* orcid.org/0000-0002-1116-6941

Complete contact information is available at: https://pubs.acs.org/10.1021/jacsau.4c00296

Author Contributions

CRediT: **Heejung Jung** conceptualization, data curation, formal analysis, investigation, methodology, writing-original draft; **Virginia Jiang** conceptualization, formal analysis, investigation, methodology, visualization, writing-original draft; **Zihang Su** investigation, methodology; **Yuta Inaba** conceptualization, investigation, methodology, writing-review & editing; **Farid Khoury** investigation, methodology; **Scott Banta** conceptualization, funding acquisition, project administration, supervision, writing-review & editing.

Notes

The authors declare no competing financial interest.

■ ACKNOWLEDGMENTS

The authors gratefully acknowledge funding through ARPA-E grant DE-AR0001340 from the U.S. Department of Energy.

■ REFERENCES

(1) Zhang, Y.; Gladyshev, V. N. Comparative genomics of trace elements: emerging dynamic view of trace element utilization and function. *Chem. Rev.* **2009**, *109*, 4828−4861.
(2) Zhang, Y.; Rump, S.; Gladyshev, V. N. Comparative genomics and evolution of molybdenum utilization. *Coord. Chem. Rev.* **2011**, *255*, 1206−1217.
(3) Bevers, L. E.; Hagedoorn, P. L.; Hagen, W. R. The bioinorganic chemistry of tungsten. *Coord. Chem. Rev.* **2009**, *253* (3−4), 269−290.
(4) Aryal, B. P.; Brugarolas, P.; He, C. Binding of ReO_4^- with an engineered MoO_4^{2-}-binding protein: towards a new approach in radiopharmaceutical applications. *J. Biol. Inorg. Chem.* **2012**, *17*, 97−106.
(5) Bevers, L. E.; Schwarz, G.; Hagen, W. R. A molecular basis for tungstate selectivity in prokaryotic ABC transport systems. *J. Bacteriol.* **2011**, *193*, 4999−5001.
(6) Hollenstein, K.; Comellas-Bigler, M.; Bevers, L. E.; Feiters, M. C.; Meyer-Klaucke, W.; Hagedoorn, P. L.; Locher, K. P. Distorted octahedral coordination of tungstate in a subfamily of specific binding proteins. *JBIC* **2009**, *14*, 663−672.
(7) Imperial, J.; Hadi, M.; Amy, N. K. Molybdate binding by ModA, the periplasmic component of the Escherichia coli mod molybdate transport system. *Biochim. Biophys. Acta- Biomembranes* **1998**, *1370*, 337−346.
(8) Coimbra, C.; Branco, R.; Morais, P. V. Efficient bioaccumulation of tungsten by *Escherichia coli* cells expressing the Sulfitobacter dubius TupBCA system. *Syst. Appl. Microbiol.* **2019**, *42*, 126001.
(9) Fernández, M.; Rico-Jiménez, M.; Ortega, C.; Daddaoua, A.; García García, A. I.; Martín-Mora, D.; Mesa Torres, N.; Tajuelo, A.; Matilla, M. A.; Krell, T. Determination of ligand profiles for *Pseudomonas aeruginosa* solute binding proteins. *Int. J. Mol. Sci.* **2019**, *20*, 5156.
(10) Hu, Y.; Rech, S.; Gunsalus, R. P.; Rees, D. C. Crystal structure of the molybdate binding protein ModA. *Nat. Struct. Biol.* **1997**, *4* (9), 703−7.
(11) Emsley, J. *Nature's Building Blocks: An A-Z Guide to the Elements*; Oxford University Press: USA, 2011; pp 446−448.
(12) Hong, T.; Liu, M.; Ma, J.; Yang, G.; Li, L.; Mumford, K. A.; Stevens, G. W. Selective recovery of rhenium from industrial leach solutions by synergistic solvent extraction. *Sep. Purif. Technol.* **2020**, *236*, 116281.
(13) Trivedi, M. V.; Laurence, J. S.; Siahaan, T. J. The role of thiols and disulfides on protein stability. *Curr. Protein Pept. Sc.* **2009**, *10*, 614−625.
(14) Karimi, M.; Ignasiak, M. T.; Chan, B.; Croft, A. K.; Radom, L.; Schiesser, C. H.; Pattison, D. I.; Davies, M. J. Reactivity of disulfide bonds is markedly affected by structure and environment: implications for protein modification and stability. *Sci. Rep.* **2016**, *6*, 38572.
(15) Wu, C.; Belenda, C.; Leroux, J.-C.; Gauthier, M. A. Interplay of chemical microenvironment and redox environment on thiol-disulfide exchange kinetics. *Chem.—Eur. J.* **2011**, *17*, 10064−10070.
(16) Yang, J.; Duan, Y.; Zhang, H.; Huang, F.; Wan, C.; Cheng, C.; Wang, L.; Peng, D.; Deng, Q. Ultrasound coupled with weak alkali cycling-induced exchange of free sulfhydryl-disulfide bond for remodeling interfacial flexibility of flaxseed protein isolates. *Food Hydrocoll.* **2023**, *140*, 108597.
(17) Depuydt, M.; Messens, J.; Collet, J. F. How proteins form disulfide bonds. *ARS* **2011**, *15* (1), 49−66.
(18) Ito, K.; Inaba, K. The disulfide bond formation (Dsb) system. *Curr. Opin. Struct. Biol.* **2008**, *18*, 450−458.
(19) Qin, L.; Liu, H.; Chen, R.; Zhou, J.; Cheng, X.; Chen, Y.; Huang, Y.; Su, Z. Effect of the flexible regions of the oncoprotein mouse double minute x on inhibitor binding affinity. *Biochem.* **2017**, *56*, 5943−5954.
(20) Manteca, A.; Alonso-Caballero, C.; Fertin, M.; Poly, S.; De Sancho, D.; Perez-Jimenez, R. The influence of disulfide bonds on the mechanical stability of proteins is context dependent. *JBC* **2017**, *292*, 13374−13380.
(21) Dopson, M.; Holmes, D. S. Metal resistance in acidophilic microorganisms and its significance for biotechnologies. *Appl. Microbiol. Biotechnol.* **2014**, *98*, 8133−8144.
(22) Jung, H.; Inaba, Y.; Banta, S. Genetic engineering of the acidophilic chemolithoautotroph Acidithiobacillus ferrooxidans. *Trends Biotechnol.* **2022**, *40*, 677−692.
(23) Jung, H.; Inaba, Y.; Jiang, V.; West, A. C.; Banta, S. Engineering polyhistidine tags on surface proteins of *Acidithiobacillus Ferrooxidans*: Impact of localization on the binding and recovery of divalent metal cations. *ACS Appl. Mater. Interfaces* **2022**, *14*, 10125−10133.
(24) Jung, H.; Kim, J.; Inaba, Y.; Moutushi, T. T.; Castaldi, M. J.; West, A. C.; Banta, S. Overexpression of AcoP in *Acidithiobacillus ferrooxidans* for enhanced copper reclamation. *ACS ES&T Eng.* **2023**, *3*, 1468−1475.
(25) Jung, H.; Su, Z.; Inaba, Y.; West, A. C.; Banta, S. Genetic modification of *Acidithiobacillus ferrooxidans* for rare-earth element recovery under acidic conditions. *Environ. Sci. Technol.* **2023**, *57*, 19902−19911.
(26) Sugio, T.; Kuwano, H.; Hamago, Y.; Negishi, A.; Maeda, T.; Takeuchi, F.; Kamimura, K. Existence of a tungsten-binding protein in *Acidithiobacillus ferrooxidans* AP19−3. *J. Biosci. Bioeng.* **2004**, *97*, 378−382.
(27) Chi, A.; Valenzuela, L.; Beard, S.; Mackey, A. J.; Shabanowitz, J.; Hunt, D. F.; Jerez, C. Periplasmic proteins of the extremophile *Acidithiobacillus ferrooxidans*: a high throughput proteomics analysis. *MCP* **2007**, *6*, 2239−2251.
(28) Kikumoto, M.; Nogami, S.; Kanao, T.; Takada, J.; Kamimura, K. Tetrathionate-forming thiosulfate dehydrogenase from the acidophilic, chemolithoautotrophic bacterium *Acidithiobacillus ferrooxidans*. *Appl. Environ. Microbiol.* **2013**, *79*, 113−120.
(29) Wang, H.; Liu, S.; Liu, X.; Li, X.; Wen, Q.; Lin, J. Identification and characterization of an ETHE1-like sulfur dioxygenase in extremely acidophilic *Acidithiobacillus* spp. *Appl. Microbiol. Biotechnol.* **2014**, *98*, 7511−7522.
(30) Bhardwaj, G.; Mulligan, V. K.; Bahl, C. D.; Gilmore, J. M.; Harvey, P. J.; Cheneval, O.; Buchko, G. W.; Pulavarti, S.; Kaas, Q.; Eletsky, A.; Huang, P. S.; Johnsen, W. A.; Greisen, P., Jr; Rocklin, G. J.; Song, Y.; Linsky, T. W.; Watkins, A.; Rettie, S. A.; Xu, X.; Carter, L. P.; Bonneau, R.; Olson, J. M.; Coutsias, E.; Correnti, C. E.; Szyperski,

T.; Craik, D. J.; Baker, D. Accurate de novo design of hyperstable constrained peptides. *Nature* **2016**, *538*, 329−335.
(31) Otrelo-Cardoso, A. R.; Nair, R. R.; Correia, M. A. S.; Cordeiro, R. S. C.; Panjkovich, A.; Svergun, D. I.; Santos-Silva, T.; Rivas, M. G. Highly selective tungstate transporter protein TupA from *Desulfovibrio alaskensis* G20. *Sci. Rep.* **2017**, *7*, 5798.
(32) Zheng, H.; Chordia, M. D.; Cooper, D. R.; Chruszcz, M.; Muller, P.; Sheldrick, G. M.; Minor, W. Validation of metal-binding sites in macromolecular structures with the CheckMyMetal web server. *Nat. Protoc.* **2014**, *9*, 156−70.
(33) Kilambi; Krishna, P.; Gray; Jeffrey, J. Rapid calculation of protein pKa values using Rosetta. *Biophys. J.* **2012**, *103*, 587−595.
(34) Sreerama, N.; Woody, R. W. Computation and Analysis of Protein Circular Dichroism Spectra. In *Methods in Enzymology*; Academic Press, 2004; Vol. *383*, pp 318−351.
(35) Baharuddin, A.; Hassan, A. A.; Othman, R.; Xu, Y.; Huang, M.; Tejo, B. A.; Yusof, R.; Rahman, N. A.; Othman, S. Dengue envelope domain III-peptide binding analysis via tryptophan fluorescence quenching assay. *Chem. Pharm. Bull.* **2014**, *62*, 947−955.
(36) Langmuir, I. The constitution and fundamental properties of solids and liquids. Part I. Solids. *J. Am. Chem. Soc.* **1916**, *38*, 2221−2295.
(37) Falagán, C.; Johnson, D. B. *Acidithiobacillus ferriphilus* sp. nov., a facultatively anaerobic iron- and sulfur-metabolizing extreme acidophile. *Int. J. Syst. Evol. Microbiol.* **2016**, *66*, 206−211.
(38) Sugio, T.; Kuwano, H.; Negishi, A.; Maeda, T.; Takeuchi, F.; Kamimura, K. Mechanism of growth inhibition by tungsten in *Acidithiobacillus ferrooxidans*. *Biosci. Biotechnol. Biochem.* **2001**, *65*, 555−562.
(39) Tuovinen, O. H.; Niemelä, S.; Gyllenberg, H. Tolerance of *Thiobacillus ferrooxidans* to some metals. *AvL* **1971**, *37*, 489−496.
(40) Inaba, Y.; West, A. C.; Banta, S. Enhanced microbial corrosion of stainless steel by *Acidithiobacillus ferrooxidans* through the manipulation of substrate oxidation and overexpression of *rus*. *Biotechnol. Bioeng.* **2020**, *117*, 3475−3485.
(41) Inaba, Y.; Xu, S.; Vardner, J. T.; West, A. C.; Banta, S. Microbially Influenced corrosion of stainless steel by *Acidithiobacillus ferrooxidans* supplemented with pyrite: Importance of thiosulfate. *Appl. Environ. Microbiol.* **2019**, *85*, No. e01381-19.
(42) Yi, G.; Zheng, D.; Song, G.-L. Surface white spot and pitting corrosion of 316 L stainless steel. *ACMM* **2021**, *68*, 1−8.
(43) Holm, R. H. Metal-centered oxygen atom transfer reactions. *Chem. Rev.* **1987**, *87*, 1401−1449.
(44) Lionetti, D.; Suseno, S.; Tsui, E. Y.; Lu, L.; Stich, T. A.; Carsch, K. M.; Nielsen, R. J.; Goddard III, W. A.; Britt, R. D.; Agapie, T. Effects of Lewis acidic metal ions (M) on oxygen-atom transfer reactivity of heterometallic Mn_3MO_4 cubane and $Fe_3MO(OH)$ and $Mn_3MO(OH)$ clusters. *Inorg. Chem.* **2019**, *58*, 2336−2345.
(45) Moltved, K. A.; Kepp, K. P. The Chemical bond between transition metals and oxygen: electronegativity, d-orbital effects, and oxophilicity as descriptors of metal-oxygen interactions. *J. Phys. Chem. C* **2019**, *123*, 18432−18444.
(46) Lawson, D. M.; Williams, C. E.; Mitchenall, L. A.; Pau, R. N. Ligand size is a major determinant of specificity in periplasmic oxyanion-binding proteins: the 1.2 Å resolution crystal structure of *Azotobacter vinelandii* ModA. *Struct.* **1998**, *6*, 1529−1539.
(47) Bailey, N.; Carrington, A.; Lott, K.; Symons, M. 55. Structure and reactivity of the oxyanions of transition metals. Part VIII. Acidities and spectra of protonated oxyanions. *J. Chem. Soc.* **1960**, 290−297.
(48) Tributsch, H. Direct versus indirect bioleaching. *Hydrometallurgy* **2001**, *59*, 177−185.

https://doi.org/10.1021/jacsau.4c00296
JACS Au 2024, 4, 2957−2965